Synthesis, Characterization, and Photovoltaic Properties of Dithienylbenzobisazole-Dithienylsilole Copolymers

Achala Bhuwalka,[1] Monique D. Ewan,[1] Jared F. Mike,[1] Moneim Elshobaki,[2,3] Brandon Kobilka,[1] Sumit Chaudhary,[4] Malika Jeffries-EL[1]

[1]Department of Chemistry Iowa State University, Ames, Iowa 50011
[2]Department of Materials Science & Engineering, Iowa State University, Ames, Iowa 50011
[3]Physics Department, Mansoura University, Mansoura, 35516, Egypt
[4]Department of Electrical and Computer Engineering, Iowa State University, Ames, Iowa 50011
Correspondence to: M. Jeffries-El (E-mail: malikaj@iastate.edu)

Received 22 September 2014; accepted 13 February 2015; published online 28 March 2015
DOI: 10.1002/pola.27603

ABSTRACT: Three conjugated polymers comprised of dioctyldithieno-[2,3-*b*:2′,3′-*d*]silole and a donor-acceptor-donor triad of either *cis*-benzbisoxazole, *trans*-benzobisoxazole or *trans*-benzobisthiazole were synthesized via the Stille cross-coupling reaction. The impact of varying the heteroatoms and/or the location within the benzobisazole moiety on the optical and electronic properties of the resulting polymers was evaluated via cyclic voltammetry and UV-Visible spectroscopy. All of the polymers have similar optical band-gaps of ~1.9 eV and highest occupied molecular orbital levels of −5.2 eV. However, the lowest unoccupied molecular orbitals (LUMO) ranged from −3.0 to −3.2 eV. Interestingly, when the polymers were used as donor materials in bulk-heterojunction photovoltaic cells with $PC_{71}BM$ as the electron-acceptor, the benzobisoxazole-based polymers gave slightly better results than the benzobisthiazole-containing polymers with power conversion efficiencies up to 3.5%. These results indicate that benzobisoxazoles are promising materials for use in OPVs. © 2015 Wiley Periodicals, Inc. J. Polym. Sci., Part A: Polym. Chem. **2015**, *53*, 1533–1540.

KEYWORDS: conjugated polymers; heteroatom containing polymer; photovoltaic cells; synthesis

INTRODUCTION Nowadays conjugated polymers (CP)s have become ubiquitous in applications such as field-effect transistors,[1] light emitting diodes,[2] photovoltaic cells,[3] and sensors.[4] CPs offer several advantages over their inorganic counterparts including solution processability potentially reducing fabrication costs, and the ability to tune their properties via organic synthesis, which enables optimization for use in specific applications. Currently, one of the most effective strategies for tuning the optical and electronic properties of CPs is through the incorporation of alternating electron donating and electron accepting comonomers within the polymer backbone.[5] This approach has afforded many materials with narrow band-gaps suitable for effective harvesting of solar energy. However, in most organic photovoltaic cells (OPV)s a bulk heterojunction is formed by using the CP as a donor material and blending it with a fullerene acceptor, such as $PC_{61}BM$ or $PC_{71}BM$. Thus, the energy levels of both materials must be well aligned for efficient electron transfer between the two materials.[6] Additionally, the morphology should be fine enough to enable efficient dissociation of electron-hair pairs at the donor:acceptor interfaces; at the same time coarser domains are also required to efficiently transport the charges to the electrodes. Although CP based OPVs are rapidly approaching the 10% power conversion efficiency (PCE) recommended for them to be competitive commercially, the development of new materials remains an important area of research.[7] In particular the development of efficient donor materials that address practical aspects of commercialization such as facile synthesis and purification of monomers, and enhanced thermal and environmental stability of the resulting material are still needed.[8]

Polybenzobisazoles are a class of polymers that are known for their exceptional thermal stability and high tensile strength of fibers spun from them.[9] For example, poly(*p*-phenylene-2,6-benzobisoxazole) is a liquid crystalline polymer based on benzo[1,2-*d*; 4,5-*d*′]benzobisoxazole that is spun into fibers commercially sold under the name

This article was published online on 28 March 2015. An error was subsequently identified. This notice is included in the online and print versions to indicate that both have been corrected on 12 April 2015.

Additional Supporting Information may be found in the online version of this article.

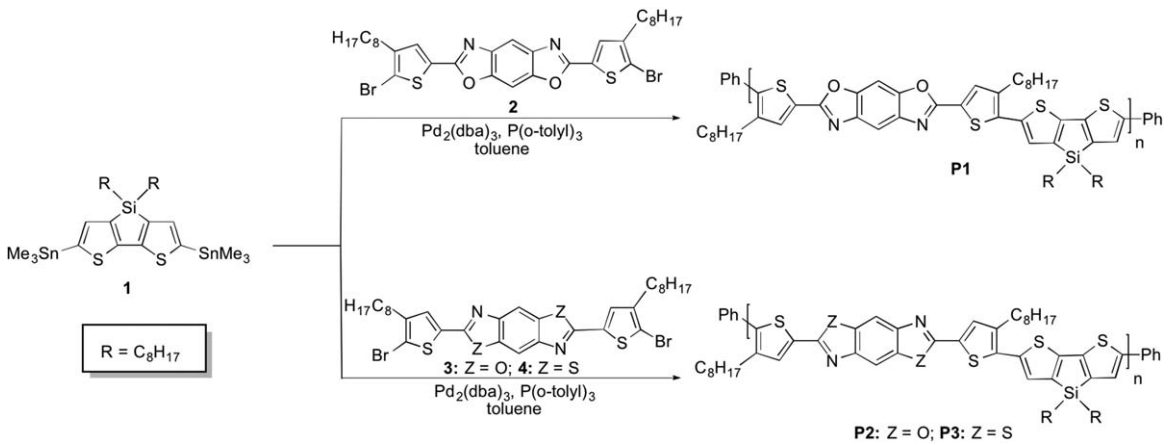

SCHEME 1 Synthesis of benzobisazole-thiophene-dithienosilole terpolymers.

Zylon®.[9(b)] Due to the previous use of polybenzobisazoles in high performance applications, all of the necessary monomers can be synthesized on industrial scale, and purified without the use of column chromatography. This is advantageous for large-scale synthesis. Furthermore, the benzobisazole ring system is electron-deficient and planar, which leads strong intermolecular interactions and good charge transport properties within polymer films.[10] Despite these advantages, the use of benzobisazoles in optoelectronic materials has been nominal due to the harsh reaction conditions used for their synthesis and their poor solubility. Traditionally, benzobisazoles are synthesized by an acid catalyzed condensation reaction at high temperatures.[9(c,d)] Such reaction conditions not only limit the types of substituents that can be on the monomer but residual acid also results in undesirable doping of the polymer and can also catalyze the degradation of the material in sunlight.[11] To address these limitations, our group has developed a mild high yielding synthesis of functional benzobisazoles via an orthoester condensation reaction.[12]

To date, there are only a few reports on the synthesis and photovoltaic properties of donor-acceptor polymers comprising benzobisazoles.[13] Ahmed et al. reported a PCE of 2.1% for a quarterthiophene benzobisthiazole polymer.[13(a)] Our group reported a PCE of only 0.6% for a related benzobisthiazole polymer, but obtained a PCE of 1.1% for the isoelectronic benzobisoxazole polymer.[13(c)] Although all of these polymers exhibited good charge carrier mobilities, they had relatively wide band gaps (1.9–2.1 eV), limiting the harvesting of solar energy. To improve on the properties of this system, we decided to evaluate the electron rich dithienosilole (DTS) moiety. This silicon bridged fused bithiophene system features two alkyl chains that impart excellent solubility to the resulting polymer, while the long C-Si bonds move the alkyl chains away from the ring system, thereby allowing for improved π-stacking. Additionally, the σ*-orbital in DTS is able to interact with the π*-orbital of the bithiophene, giving a conjugated, planar system further increasing π-stacking interactions and the long-range order.[14] Furthermore, DTS has a lower-lying (LUMO) and highest occupied molecular orbital (HOMO) than other bithiophene derivatives, which can reduce the polymer band gap and increase the open circuit voltage (V_{oc}) of the devices fabricated from them affording PCEs as high as 7.3%.[15] Ahmed et al. reported a PCE of 2.1% for a BHJ device using a dithienosilole-dithienylbenzobisthiazole polymer as the donor and $PC_{71}BM$ as the acceptor.[13(b)] Since, our previous results indicate that polymers incorporating the benzobisoxazole moiety exhibited higher V_{oc} and PCE in comparison to the analogous benzobisthiazole polymers, we set out to evaluate the optical and electronic properties of a series of polymers containing DTS and the isomeric benzo[1,2-*d*; 5,4-*d'*]bisoxazole (*cis*-BBO) and benzo[1,2-*d*; 4,5-*d'*]bisoxazole (*trans*-BBO) and the isoelectronic benzo[1,2-*d*; 4,5-*d'*]bisthiazole (*trans*-BBZT). We note that could not include the *cis*-BBZT polymer in our studies as the synthesis of the required starting material, 4,6-diamino-1,3-benzenedithiol has not been reported in the modern era. Our attempts to prepare this compound according to literature procedure yield different products from the reports. Furthermore, all efforts to synthesize this compound in our labs using new approaches have been unsuccessful.

EXPERIMENTAL

Materials and General Experimental Details

Tetrahydrofuran and toluene were dried using an Innovative Technologies solvent purification system. Air and moisture sensitive reactions were performed using standard Schlenk techniques. Solvents used for palladium-catalyzed reactions were deoxygenated prior to use by bubbling a stream of argon through the solvent with vigorous stirring for 30 to 60 min. All chemical reagents were purchased from commercial sources and used without further purification unless otherwise noted. SiliaMetS® Cysteine was purchased from SiliCycle, Inc. 4,4-Dioctyl-2,6-*bis*(trimethylstannyl)-4*H*-silolo[3,2-*b*:4,5-*b'*]dithiophene **(1)**,[16] 2,6-*bis*(4-octylthiophen-2-yl)benzo[1,2-*d*; 5,4-*d'*]bisoxazole **(2)**, 2,6-*Bis*(4-octylthiophen-2-yl)benzo[1,2-*d*; 4,5-*d'*]bisoxazole **(3)**, and 2,6-*Bis*(4-octylthiophen-2-yl)benzo[1,2-*d*; 4,5-*d'*]bisthiazole **(4)** were synthesized according to literature procedures.[12(b)]

General Polymerization Procedure

A mixture of **1** and the respective benzobisazole, 2 mol % *tris*(dibenzylideneacetone)dipalladium(0), 8 mol % *tris*-o-tolyphosphine in 7 mL of degassed toluene was added to a round bottom flask equipped with a reflux condenser and an argon inlet. The mixture was allowed to reflux for 12 to 36 h before it was end capped by addition of trimethylphenyl tin followed by iodobenzene. The reaction was then quenched by pouring into 100 mL of cold methanol. The precipitated polymer was filtered into a cellulose extraction thimble and purified by Soxhlet extraction with methanol to remove residual palladium followed by acetone and hexanes to remove the lower molecular weight material. The polymers were then obtained using $CHCl_3$ as the extraction solvent. Functionalized silica (SiliaMetS® Cysteine) was added to the chloroform fraction and the solution was allowed to stir overnight at 50 °C. The chloroform fraction was then filtered through a bed of Celite and the solvent was removed under vacuum. The polymer was then reprecipitated in methanol, filtered and dried in the vacuum oven overnight.

Poly(2-(5-(4,4-dioctyl-4H-silolo[3,2-b:4,5-b']dithiophen-2-yl)-4-octylthiophen-2-yl)-6-(4-octylthiophen-2-yl)benzo[1,2-d:5,4-d']bis(oxazole))(P1)

Polymer was obtained as dark red solid (298 mg, 89% yield) from **2** and **1** (250 mg, 0.33 mmol); GPC: M_n =11.6 kDa, M_w = 26.2kDa, PDI = 2.3.

Poly(2-(5-(4,4-dioctyl-4H-silolo[3,2-b:4,5-b']dithiophen-2-yl)-4-octylthiophen-2-yl)-6-(4-octylthiophen-2-yl)benzo[1,2-d:4,5-d']bis(oxazole))(P2)

Polymer obtained as a deep red solid (275 mg, 83% yield) from **3** (237 mg, 0.33 mmol) and **1** (250 mg, 0.33 mmol); GPC: M_n = 12.4 kDa, M_w = 31.7 kDa, PDI = 2.6.

Poly(2-(5-(4,4-dioctyl-4H-silolo[3,2-b:4,5-b']dithiophen-2-yl)-4-octylthiophen-2-yl)-6-(4-octylthiophen-2-yl)benzo[1,2-d:4,5-d']bis(thiazole))(P3)

Polymer obtained as a deep red-purple solid (273 mg, 79% yield) starting with **4** (248 mg, 0.33 mmol) and **1** (250 mg, 0.33 mmol); GPC: M_n = 9.5 kDa, M_w = 20.8 kDa, PDI = 2.2.

Device Fabrication and Characterization

ITO-coated glass substrates were cleaned sequentially by ultrasonication in acetone, methanol, and isopropanol, followed by O_2 plasma exposure for 5 min. PEDOT:PSS aqueous solution was passed through a 0.45 μm PVDF filter, and then spin-coated on the ITO substrate at 4000 rpm for 60 s and dried in a vacuum oven at 120 °C for 1 h. The thickness of PEDOT:PSS layer was approximately 40 nm. All devices were fabricated in a glove box filled with argon. 50 mg/mL $PC_{71}BM$ in *o*-DCB was prepared by ultrasonic mixing for 1 h and filtered with a 0.45 μm PTFE filter prior to use. The polymers **P1**, **P2**, and **P3** were dissolved in *o*-DCB at 90 °C to yield 10 mg/mL polymer/*o*-DCB solution. The hot solution was quickly filtered with a 0.45 μm PTFE filter before cooling down to room temperature. Photovoltaic devices with a configuration of ITO/PEDOT:PSS/ Polymer:$PC_{71}BM$/Ca/Al were fabricated at a 1:2 weight ratio of polymer to $PC_{71}BM$ and a total solution concentration of 21 mg/mL. These devices were evaluated with and without the solvent additive, 1,8-diiodooctane (DIO). A cathode was prepared by sequentially depositing a Ca film (20 nm) and an Al film (100 nm) through a shadow mask. The photovoltaic devices had an area of 0.10 ± 0.01 cm^2 and were tested under simulated AM 1.5 G irradiation (100 mW cm^{-2}, calibrated with Daystar Meter) using a SoLux Solar Simulator, and the current–voltage (*I–V*) curves were measured using a Keithley 2400 multisource meter. A Veeco Digital Instruments atomic force microscope (AFM) was used to map the surface profile of the investigated thin films. Both the surface roughness and phase images were captured simultaneously at scan rate and size of 0.5 Hz and 3 μm × 3 μm, respectively. The images were analyzed using Nanotec Electronica WSxM software.[17]

TABLE 1 Physical Characterization of P1–P3

Polymer	Yield[a] (%)	M_n[b] (kDa)	PDI[b]	DP_n	T_d (°C)[c]
P1	89	11.6	2.3	12	308
P2	83	12.4	2.6	12	306
P3	55	9.5	2.2	9	315

[a] Isolated yield.
[b] Determined by GPC in $CHCl_3$ using polystyrene standards.
[c] 5% weight loss temperature by TGA in air.

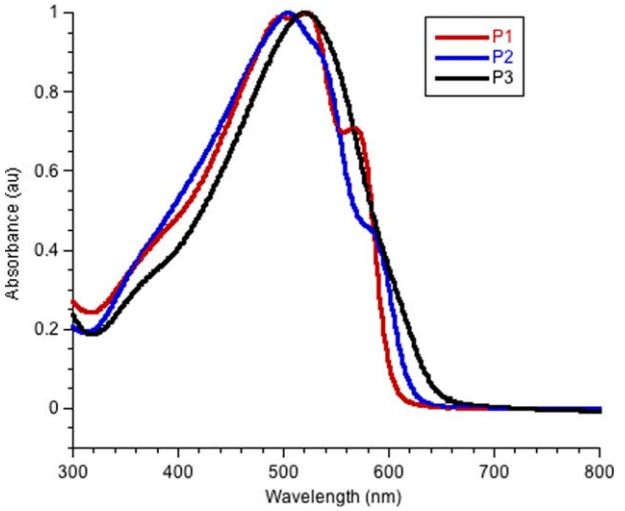

FIGURE 1 UV-Vis absorption spectra of **P1–P3** in dilute chloroform solutions. [Color figure can be viewed in the online issue, which is available at wileyonlinelibrary.com.]

RESULTS AND DISCUSSION

Synthesis

We utilized a monomer composed of a benzobisazole moiety placed between two brominated thiophene rings with the alkyl chains facing away from the benzene core for the polymer synthesis. The thiophene rings serve as π spacers whereas the octyl chains aid solubility. The halogens on the thiophene rings provide a handle for transition metal catalyzed cross-coupling reactions, while avoiding potential ring

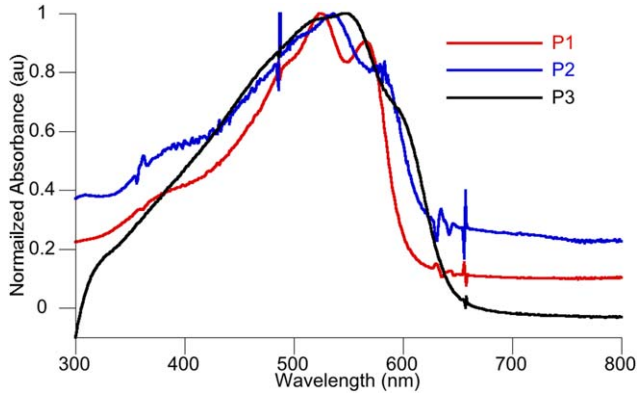

FIGURE 2 UV-Vis absorption spectra of **P1–P3** as thin films. Thin films were spun from polymer solutions in 1:1 (v/v) $CHCl_3$:*o*DCB (2 mg/mL). [Color figure can be viewed in the online issue, which is available at wileyonlinelibrary.com.]

opening reactions that can occur during palladium insertion at the second position of benzazoles.[18] The synthetic routes toward the polymers are outlined in Scheme 1. The Stille cross-coupling polymerization of 4,4-dioctyl-2,6-*bis*(trimethylstannyl)−4*H*-silolo[3,2-*b*:4,5-*b′*]bithiophene **1**[16] with either 2,6-*bis*(4-octylthiophen-2-yl)-benzo[1,2-*d*; 5,4-*d′*]bisoxazole **2**, 2,6-*bis*(4-octylthiophen-2-yl)-benzo[1,2-*d*; 4,5-*d′*]bisoxazole **3**, or 2,6-*bis*(4-octylthiophen-2-yl)-benzo[1,2-*d*; 4,5-*d′*]bisthiazole **4**[12(b)] afforded polymers **P1**, **P2,** and **P3**, respectively. All the polymers exhibited reasonable solubility (∼10 mg/mL) in standard organic solvents, such as THF, *m*-cresol, and chloroform at room temperature, enabling characterization by gel permeation chromatography (GPC). The weight-averaged (M_w), number-averaged (M_n) molecular weights and polydispersity index (PDI) as estimated using GPC are summarized in Table 1. The number averaged degree of polymerization (DP_n) for the polymers was determined to range from 9 to 12. Unfortunately, the limited solubility of the polymers the disproportionate ratio of alkyl to aryl protons and the generally lower signal to noise obtained for quarternary protons prevented analysis by ^{1}H NMR spectroscopy. Thermogravimetric analysis (TGA) revealed that all polymers were thermally stable with 5% weight loss onsets occurring above 300 °C under air (Supporting Information Fig. S6). None of the polymers exhibited any glass transitions as shown by differential scanning calorimetry (DSC) (Supporting Information Fig. S7). The results are summarized in Table 1.

Optical and Electrochemical Properties

The optical properties of the polymers were investigated using UV-Visible absorption spectroscopy in solution and solid state. The normalized absorbance spectra of the polymer solutions in dilute chloroform solution and in the solid state are shown in Figures 1 and 2, respectively. The data is summarized in Table 2. In solution, the λ_{max} of all the polymers are similar. However, **P1** and **P2** have small shoulders arising from aggregation in polymer backbone,[13(a)] whereas **P3** exhibits a single, featureless absorbance band. As thin films, the λ_{max} values for **P1**, **P2,** and **P3** are 524 nm, 536 nm, and 549 nm, respectively. These absorbance spectra are slightly broader than the corresponding solution spectra, resulting in bathochromic shifts of 2 nm to 30 nm in the absorption maximum. This suggests a slight increase in the backbone planarization and π- stacking in the solid state.[19] The film λ_{max} of **P3** is the same as that reported by Ahmed et al. for a similar polymer which had branched alkyl chains on the dithienosilole unit and the alkyl chain on the thiophenes flanking the benzobisthiazole moiety was facing inwards.[13(b)] The solution and thin film λ_{max} values of **P1–P3** are bathochromically shifted by 70 to 95 nm relative to our previous reported polymers which employed bithiophene as the donor.[13(c)] This can be attributed to the fused dithienosilole ring system which can lead to a more rigid, coplanar backbone thereby increasing the effective π-conjugation length, decreasing the band gap and red-shifting the absorbance spectra.

The optical band gaps for **P1–P3** were estimated from the onset wavelength of the polymers films and range from 1.9 to 2.0 eV. As expected, these band-gaps are slightly narrower than those reported previously for the benzobisazole-quarterthiophene system which ranged from 2.1 eV to 2.2 eV.[13(c)] This further demonstrates that using a stronger fused electron-donating comonomer was beneficial in narrowing the band gap.

Using cyclic voltammetry, the electrochemical properties of the polymers were evaluated and the results are summarized

TABLE 2 Electronic and Optical Properties of Benzobisazole-Thiophene-Dithienosilole Terpolymers

Polymer	Solution	Film							
	$\lambda_{max}^{soln}(nm)$	$\lambda_{max}^{film}(nm)$	λonset (nm)	E_g^{opt}(eV)[a]	E_g^{EC}(eV)[b]	E_{onset}^{ox}	E_{onset}^{red}	LUMO (eV)[c]	HOMO (eV)[d]
P1	522	524	610	2.0	2.2	0.4	−1.8	−3.0	−5.2
P2	505	536	640	1.9	2.0	0.4	−1.6	−3.2	−5.2
P3	520	549	650	1.9	–	0.5	–	–	−5.2

Electrochemical properties were measured using a three-electrode cell (electrolyte: 0.1 mol/L $TBAPF_6$ in acetonitrile) with an Ag/Ag^+ reference electrode, a platinum auxiliary electrode, and a platinum button electrode as the working electrode. Reported values are referenced to Fc/Fc^+. Polymer films were drop cast on to the working electrode from an *o*-DCB solution of **P1–P3**. No reduction peak was seen for **P3**.

[a] Estimated from the optical absorption edge.
[b] Estimated from HOMO-LUMO.
[c] LUMO = $-4.8-(E^{red}{}_{onset})$ (eV).
[d] HOMO = $-4.8-(E^{ox}{}_{onset})$ (eV).

TABLE 3 Photovoltaic Device Performance of **P1–P3** with $PC_{71}BM$

Polymer	Additive (% DIO)	J_{SC} (mA/cm^2)	V_{OC} (V)	FF	PCE (%)	Max PCE (%)	R_{SH} (Ω cm^2)
P1	None	8.07 ± 5.89	0.69 ± 0.03	0.40 ± 0.05	2.01 ± 1.00	3.51	457 ± 259
P1	0.5	3.14 ± 0.07	0.69 ± 0.02	0.49 ± 0.02	1.08 ± 0.02	1.11	1,656 ± 127
P1	2.5	4.00 ± 0.21	0.65 ± 0.05	0.46 ± 0.01	1.20 ± 0.20	1.34	982 ± 134
P2	None	5.13 ± 1.49	0.71 ± 0.01	0.46 ± 0.04	1.67 ± 0.44	2.57	818 ± 209
P2	0.5	4.47 ± 0.07	0.71 ± 0.01	0.46 ± 0.01	1.43 ± 0.03	1.45	792 ± 34
P2	2.5	4.80 ± 0.04	0.69 ± 0.01	0.42 ± 0.01	1.39 ± 0.02	1.42	708 ± 37
P3	None	5.27 ± 3.11	0.66 ± 0.01	0.44 ± 0.08	1.44 ± 0.48	2.15	944 ± 455
P3	0.5	3.78 ± 0.13	0.68 ± 0.02	0.46 ± 0.01	1.17 ± 0.03	1.21	970 ± 40
P3	2.5	4.23 ± 0.15	0.67 ± 0.01	0.43 ± 0.01	1.22 ± 0.03	1.25	835 ± 146

Photovoltaic devices with a configuration of ITO/PEDOT:PSS/Polymer:$PC_{71}BM$/Ca/Al were fabricated at a 1:2 weight ratio of polymer to $PC_{71}BM$ and a total solution concentration of 21 mg/mL. DIO was used as the additive (% v/v).

in Table 2. **P1** and **P2** showed reproducible oxidation and reduction processes, whereas **P3** only showed a clear wave during the oxidation cycle (Supporting Information Fig. S5). The HOMO levels were all ranged from −5.2 to −5.3 eV and were estimated using the absolute energy level of ferrocene/ferrocenium (Fc/Fc^+) as 4.8 eV under vacuum and the onsets of oxidation.[20] These are deep enough to provide good air stability.[6(b)] Similarly, the LUMO levels of −3.0 eV and −3.2 eV were estimated using the onsets of reduction for the BBO polymers **P1** and **P2**, respectively. The *trans*-BBZT polymer **P3** did not exhibit a measurable reduction wave. These results indicate that the HOMO level of these polymers are unaffected by changing the configuration of the oxygen atoms or replacing them with sulphur. In contrast, switching the oxygen from the *cis*- to the *trans*-configuration reduced the LUMO level by ∼0.2 eV. The LUMO levels for all of the polymers are also lower than those of their quarterthiophene counterparts.[13(c)] Thus replacing the bithiophene with DTS was beneficial. The difference between the electrochemical band gaps of **P1** and **P2** and their optical band gaps is typical for these measurements due to the energy barrier associated with the interface of the polymer film and the electrode surface.[20,21]

Photovoltaic Properties

The OPV performances of the polymers was evaluated using photovoltaic devices with a configuration of ITO/PEDOT:PSS/**Polymer**:$PC_{71}BM$/Ca/Al and a 1:2 weight ratio of polymer to $PC_{71}BM$ with a total solution concentration of 21 mg/mL. These devices were evaluated with and without the solvent additive, DIO. The photovoltaic parameters including short circuit current density (J_{SC}), open circuit voltage (V_{OC}), fill factor (FF), and power conversion efficiency (PCE) are listed in Table 3. The current density–voltage (*J–V*) curves of **P1**:$PC_{71}BM$, **P2**:$PC_{71}BM$, and **P3**:$PC_{71}BM$ photovoltaic devices under AM 1.5 G illumination (100 mW/cm^2) are shown in Figure 3. We were able to obtain maximum PCE values of 2.47, 3.51, and 2.15 for **P1**, **P2**, and **P3**, respectively. However, we were unable to obtain these values reproducibly in subsequent runs. This is indicative of the difficulty in obtaining ideal nanoscale morphology within the polymer:fullerene blends. On average the devices based on the benzobisoxazole polymers **P1** and **P2** had similar

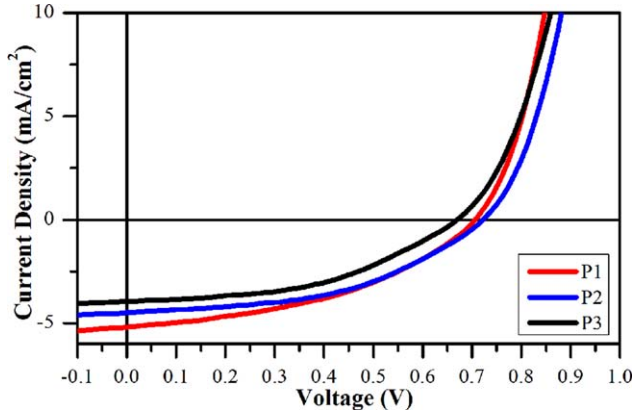

FIGURE 3 Current density–voltage *(J–V)* curves of polymer:$PC_{71}BM$, photovoltaic devices under AM 1.5 G illumination (100 mW cm^{-2}). [Color figure can be viewed in the online issue, which is available at wileyonlinelibrary.com.]

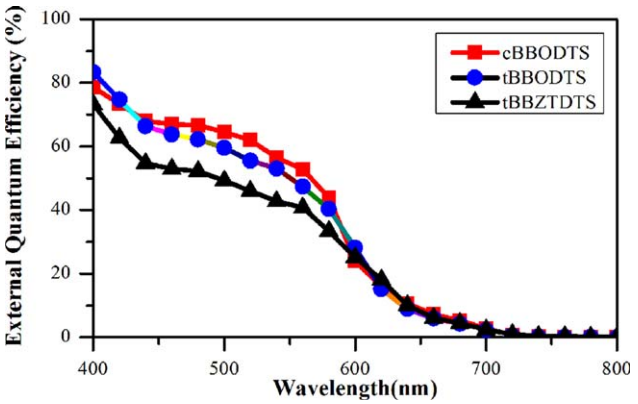

FIGURE 4 The external quantum efficiency of polymer:$PC_{71}BM$, photovoltaic devices under AM 1.5 G illumination (100 mW cm^{-2}). [Color figure can be viewed in the online issue, which is available at wileyonlinelibrary.com.]

TABLE 4 Mobility of **P1–P3** Hole-Only Devices and AFM Data of Polymer: $PC_{71}BM$ Blends

Polymer	μ_h ($cm^2\ V^{-1}\ s^{-1}$)	RMS Roughness (nm)
P1	8.04E-06	1.08
P2	5.06E-06	0.97
P3	2.34E-06	1.30

performance with PCEs of ~1.5% without the use of solvent additives. Whereas, the performance of the devices made from the benzobisthiazole polymer **P3** were slightly lower with a PCEs of 1.22%. We also evaluated the use of DIO as a solvent additive,[22] but only observed a nominal improvement in the PCE for **P3**, and a minor decrease in the performance of **P1** and **P2**. In general, the performances of these devices were modest as a result of both J_{SC} and V_{OC} and moderate FF. The external quantum efficiency (EQE) curves for the best devices are shown in Figure 4. All of the devices had broad photoresponses between 400 and 690 nm, with a maximum EQE of 79% at 400 nm, 83% at 400 nm, and 73% at 400 nm, for **P1**, **P2**, and **P3**, respectively. These overall performance of these polymers represent a modest improvement over our previously results on poly(quarterthiophene benzobisazoles), in which the best performance was a PCE of 1.14% for the *trans*-BBO polymer.[13(c)] The OPV performance of **P3** is comparable to that reported by Ahmed et al. for a related benzobisthiazole polymer, poly[(4,4′-*bis*(2-ethylhexyl)dithieno[3,2-*b*:2′,3′-*d*]silole)−2,6-diyl-alt-(2,5-*bis*(3-dodecylthiophen-2-yl)benzo[1,2-*d*;4,5-*d*′]bisthiazole)] (PBTEHS), which had a PCE of 1.24% that increased to 2.02% with the use of additives.[13(b)] Although PBTEHS and **P3** have different substituents on both the flanking thiophenes and benzodithiophene, the similarities in their initial performance but different behavior upon the addition of the co-solvents suggest that the polymers' structure has a negative impact on the morphology of the blends thin film.

The hole mobilities of the polymers were examined using the space-charge-limited current (SCLC) method with a hole only device structure of ITO/PEDOT:PSS/Polymer/Al and are summarized in Table 4.[23] The mobilites were calculated according to Eq 1:

$$J_{SCLC} = \frac{9\varepsilon_0\varepsilon_r\mu_h V^2}{8L^3} \quad (1)$$

in which $\varepsilon_0\varepsilon_r$ is the permittivity of the polymer, μ_h is the carrier mobility, and L is the device thickness.[24] The mobilities of the polymers were on the same order of magnitude as each other, with **P3** having the lowest mobility. This is consistent with the OPV data, with **P3** giving the worst performance, by only by a small margin.

Film Morphology

The surface roughness and phase distribution of the three polymer systems were studied by atomic force microscopy (AFM) (Fig. 5). The AFM height images reveal smooth topography for all three polymers with root-mean square (RMS) surface roughness values less than 1.30 nm (Table 4). In the phase images, **P1**:$PC_{71}BM$ and **P2**:$PC_{71}BM$ thin-films show a bi-phasic distribution. However, the phase image of **P3**:$PC_{71}BM$ thin film is notably different and shows a strong vertical phase separation, which hampers both exciton

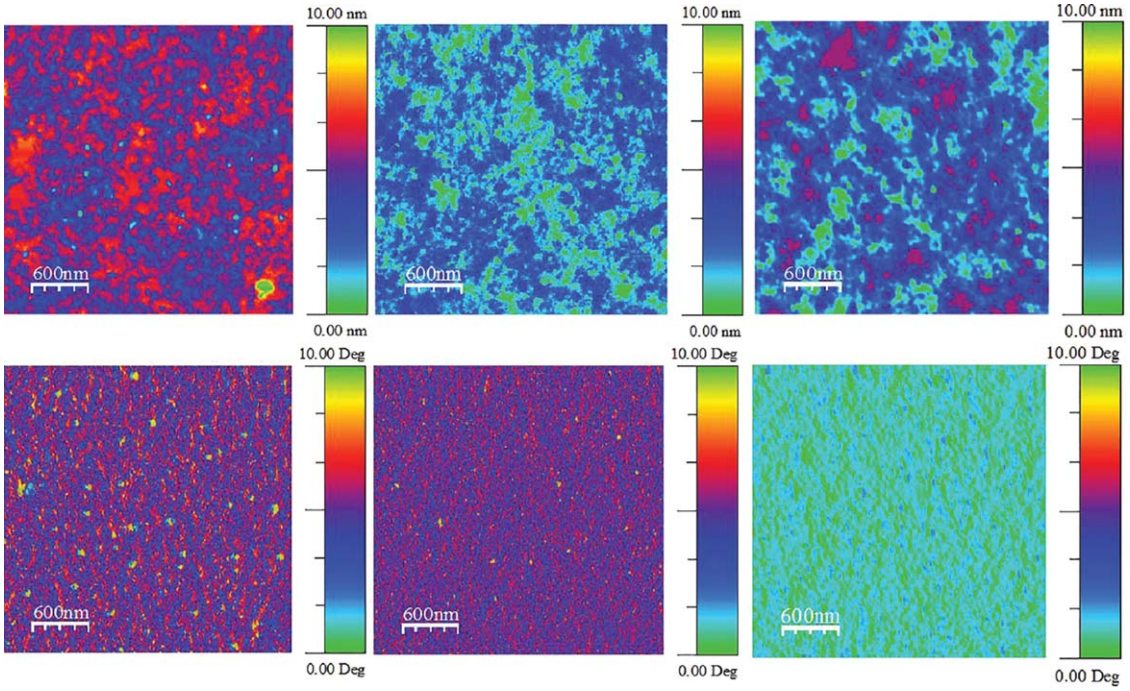

FIGURE 5 AFM height (top) and phase (bottom) images at 3 μm × 3 μm of devices with polymer:$PC_{71}BM$ blends at a 1:2 weight ratio. From left to right: **P1**:$PC_{71}BM$, **P2**:$PC_{71}BM$ and **P3**:$PC_{71}BM$.

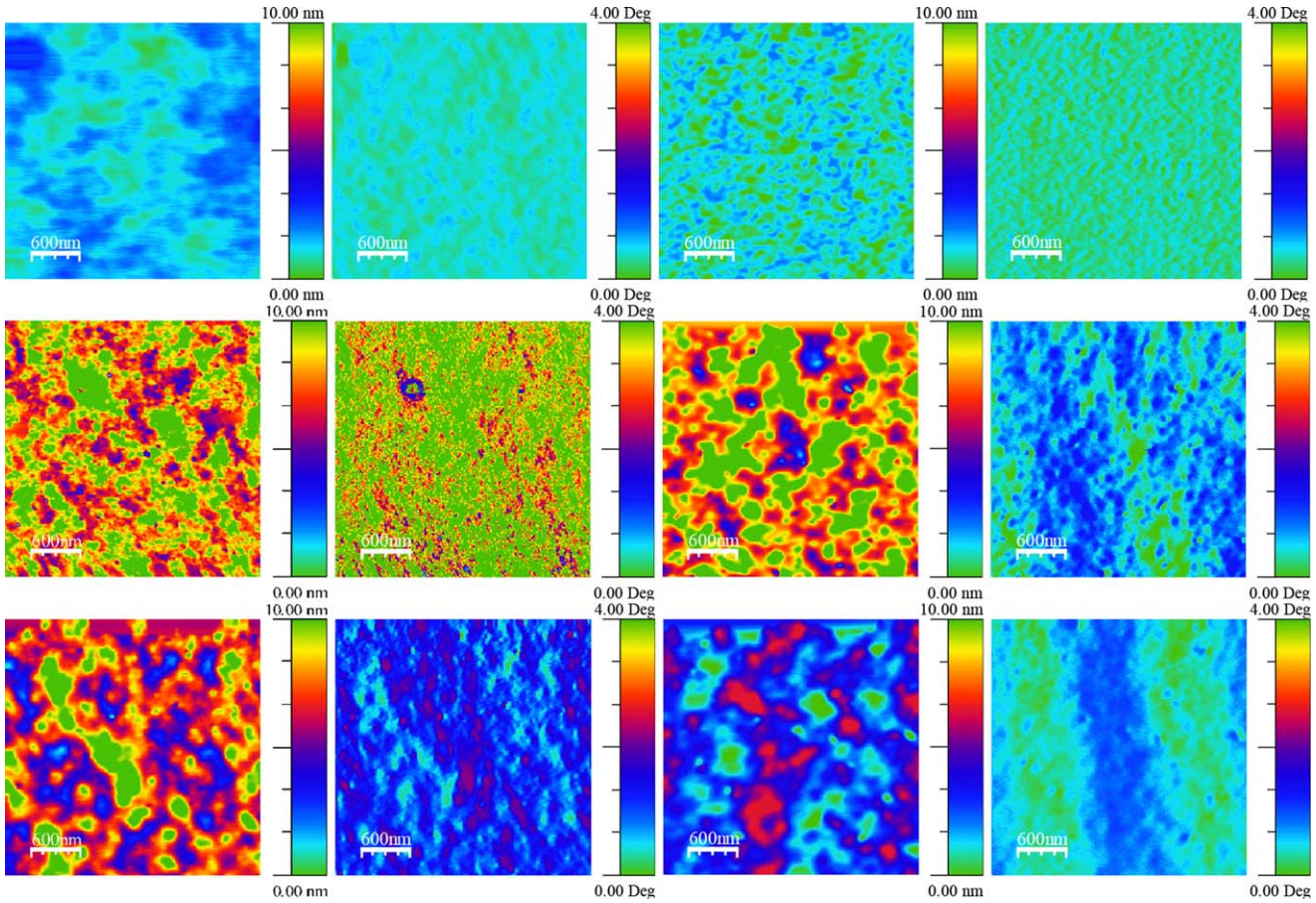

FIGURE 6 AFM height (first and third column) and phase (second and fourth column) of **P1**:$PC_{71}BM$ blends and **P2**:$PC_{71}BM$ blends, respectively. Images at 3 μm × 3 μm of devices with a 1:2 weight ratio. From top to bottom: control. 0.5% DIO and 2.5% DIO.

dissociation and charge transport, and explainsthe poorest performance of the **P3** based devices. It is known that the BBZT containing polymers have poorer solubility than the BBO based ones.[12(b),13(c)] The reduced solubility of **P3** relative to **P1** and **P2** strongly affects the polymer/fullerene intermixing, and potentially increases tendency for aggregation.

The surface morphology of the **P1**:$PC_{71}BM$ and **P2**:$PC_{71}BM$ thin films with varying amounts of DIO (0, 0.5, and 2.5 vol %) was also investigated by AFM (Fig. 6). The RMS surface roughness values of the films with 0.5 vol % (1.86 nm for **P1** and 2.05 nm for **P2**) and 2.5 vol % (2.12 nm for **P1** and 1.56 nm for **P2**) DIO additives were larger than the films processed without any additives (0.47 nm for **P1** and 0.48 nm for **P2**). On the other hand, AFM phase images of the DIO-treated thin films display larger domain sizes, which indicate the existence of large polymer aggregates. This suppresses the exciton dissociation, short-circuit-current, and consequently the power conversion efficiency of the DIO-treated devices (Table 3). While the role of the solvent additive generally is to facilitate the crystallization of the polymer around the fullerene,[25] in the case of these polymers the large aggregates obtained are not favorable. In the future, different solvent additives will be investigated to further optimize the OPV performance of polybenzobisazoles-based solar cells.

CONCLUSIONS

In summary, a series of donor-acceptor copolymers based on dithienylbenzobisazole and dithieno[3,2-*b*:2′,3′-*d*]silole were synthesized in an effort to improve the OPV performance of benzobisazole polymers. Although the polymers differed in the location and/or nature of the heteroatoms within the benzobisazole moiety they had identical HOMO levels (−5.2 eV) and fairly similar LUMO levels (−3.0 to 3.2 eV). The use of the DTS monomer had only a moderate effect on the band gap of these polymers. However, these materials did outperform our previously reported benzobisazoles. Furthermore our data indicates that among this series, benzobisoxazole based polymers are the most promising due to improved solubility and thin film formation. Research is ongoing in our lab to further improve upon the properties of this class of polymers.

ACKNOWLEDGMENTS

We thank the National Science Foundation (DMR-0846607, ECCS-1055930) for support of this work. We also thank the

National Science Foundation Materials Research Facilities Network (DMR-0820506) and Polymer-Based Materials for Harvesting Solar Energy, an Energy Frontier Research Center funded by the U.S. Department of Energy, Office of Science, Office of Basic Energy Sciences under Award Number DE-SC0001087 for support of the device fabrication. Some of the OPV work was performed at the ISU Microelectronics Research Center. The Iowa State University (ISU), the Institute for Physical Research and Technology provided MDE with a Catron Fellowship. M. Elshobaki thanks the financial support from the Egyptian government (scholarship # GM915).

REFERENCES AND NOTES

1 (a) A. Facchetti, *Mater. Today* **2007**, *10*, 28; (b) Z. Bao, A. J. Lovinger, *Chem. Mater.* **1999**, *11*, 2607.

2 (a) R. H. Friend, R. W. Gymer, A. B. Holmes, J. H. Burroughes, R. N. Marks, C. Taliani, D. D. C. Bradley, D. A. Dos Santos, J. L. Bredas, M. Logdlund, W. R. Salaneck, *Nature* **1999**, *397*, 121; (b) C. W. Tang, S. A. VanSlyke, *Appl. Phys. Lett.* **1987**, *51*, 913; (c) A. C. Grimsdale, K. Leok Chan, R. E. Martin, P. G. Jokisz, A. B. Holmes, *Chem. Rev.* **2009**, *109*, 897.

3 (a) C. W. Tang, *Appl. Phys. Lett.* **1986**, *48*, 183; (b) A. Facchetti, *Chem. Mater.* **2011**, *23*, 733; (c) S. Günes, H. Neugebauer, N. S. Sariciftci, *Chem. Rev.* **2007**, *107*, 1324.

4 (a) D. T. McQuade, A. E. Pullen, T. M. Swager, *Chem. Rev.* **2000**, *100*, 2537; (b) S. W. Thomas, G. D. Joly, T. M. Swager, *Chem. Rev.* **2007**, *107*, 1339.

5 (a) H. A. M. van Mullekom, J. A. J. M. Vekemans, E. E. Havinga, E. W. Meijer, *Mater. Sci. Eng. R Rep.* **2001**, *32*, 1; (b) E. E. Havinga, W. ten Hoeve, H. Wynberg, *Polym. Bull.* **1992**, *29*, 119; (c) E. E. Havinga, W. ten Hoeve, H. Wynberg, *Synth. Met.* **1993**, *55*, 299.

6 (a) L. J. A. Koster, V. D. Mihailetchi, P. W. M. Blom, *Appl. Phys. Lett.* **2006**, *88*, 093511; (b) B. C. Thompson, Y.-G. Kim, J. R. Reynolds, *Macromolecules* **2005**, *38*, 5359.

7 (a) H. J. Son, B. Carsten, I. H. Jung, L. Yu, *Energy Environ. Sci.* **2012**, *5*, 8158; (b) G. Dennler, M. C. Scharber, C. J. Brabec, *Adv. Mater.* **2009**, *21*, 1323; (c) J. Kalowekamo, E. Baker, *Solar Energy* **2009**, *83*, 1224.

8 R. Po, A. Bernardi, A. Calabrese, C. Carbonera, G. Corso, A. Pellegrino, *Energy Environ. Sci.* **2014**, *7*, 925.

9 (a) M. A. Wolak, B. B. Jang, L. C. Palilis, Z. H. Kafafi, J. *Phys. Chem. B* **2004**, *108*, 5492; (b) J. F. Wolfe, In *Encyclopedia of Polymer Science and Engineering*; Wiley: New York, **1988**; Vol. *11*, pp 601; (c) J. F. Wolfe, F. E. Arnold, *Macromolecules* **1981**, *14*, 909; (d) J. F. Wolfe, B. H. Loo, F. E. Arnold, *Macromolecules* **1981**, *14*, 915.

10 (a) M. M. Alam, S. A. Jenekhe, *Chem. Mater.* **2002**, *14*, 4775; (b) H. Pang, F. Vilela, P. J. Skabara, J. J. W. McDouall, D. J. Crouch, T. D. Anthopoulos, D. D. C. Bradley, D. M. de Leeuw, P. N. Horton, M. B. Hursthouse, *Adv. Mater.* **2007**, *19*, 4438; (c) I. Osaka, K. Takimiya, R. D. McCullough, *Adv. Mater.* **2010**, *22*, 4993.

11 B. Song, Q. Fu, L. Ying, X. Liu, Q. Zhuang, Z. Han, *J. Appl. Polym. Sci.* **2012**, *124*, 1050.

12 (a) J. F. Mike, J. J. Inteman, A. Ellern, M. Jeffries-El, *J. Org. Chem.* **2009**, *75*, 495; (b) J. F. Mike, J. J. Intemann, M. Cai, T. Xiao, R. Shinar, J. Shinar, M. Jeffries-EL, *Polym. Chem.* **2011**, *2*, 2299; (c) J. F. Mike, A. J. Makowski, M. Jeffries-El, *Org. Lett.* **2008**, *10*, 4915.

13 (a) E. Ahmed, F. S. Kim, H. Xin, S. A. Jenekhe, *Macromolecules* **2009**, *42*, 8615; (b) E. Ahmed, S. Subramaniyan, F. S. Kim, H. Xin, S. A. Jenekhe, *Macromolecules* **2011**, *44*, 7207; (c) A. Bhuwalka, J. F. Mike, M. He, J. J. Intemann, T. Nelson, M. D. Ewan, R. A. Roggers, Z. Lin, M. Jeffries-El, *Macromolecules* **2011**, *44*, 9611; (d) A. V. Patil, H. Park, E. W. Lee, S.-H. Lee, *Synth. Met.* **2010**, *160*, 2128; (e) M. Tsuji, A. Saeki, Y. Koizumi, N. Matsuyama, C. Vijayakumar, S. Seki, *Adv. Funct. Mater.* **2014**, *24*, 28; (f) A. Saeki, M. Tsuji, S. Yoshikawa, A. Gopal, S. Seki, *J. Mater. Chem. A* **2014**, *2*, 6075; (g) S. Subramaniyan, F. S. Kim, G. Ren, H. Li, S. A. Jenekhe, *Macromolecules* **2012**, *45*, 9029.

14 H.-Y. Chen, J. Hou, A. E. Hayden, H. Yang, K. N. Houk, Y. Yang, *Adv. Mater.* **2010**, *22*, 371.

15 T.-Y. Chu, J. Lu, S. Beaupré, Y. Zhang, J.-R. Pouliot, S. Wakim, J. Zhou, M. Leclerc, Z. Li, J. Ding, Y. Tao, *J. Am. Chem. Soc.* **2011**, *133*, 4250.

16 L. Huo, Y. Zhou, Y. Li, *Macromol. Rapid Commun.* **2008**, *29*, 1444.

17 I. Horcas, R. Fernández, J. M. Gómez-Rodríguez, J. Colchero, J. Gómez-Herrero, A. M. Baro, *Rev. Sci. Instrum.* **2007**, *78*, 013705.

18 R. S. Sanchez, F. A. Zhuravlev, *J. Am. Chem. Soc.* **2007**, *129*, 5824.

19 H. Kokubo, T. Sato, T. Yamamoto, *Macromolecules* **2006**, *39*, 3959.

20 C. M. Cardona, W. Li, A. E. Kaifer, D. Stockdale, G. C. Bazan, *Adv. Mater.* **2011**, *23*, 2367.

21 S. Admassie, O. Inganäs, W. Mammo, E. Perzon, M. R. Andersson, *Synth. Met.* **2006**, *156*, 614.

22 J. K. Lee, W. L. Ma, C. J. Brabec, J. Yuen, J. S. Moon, J. Y. Kim, K. Lee, G. C. Bazan, A. J. Heeger, *J. Am. Chem. Soc.* **2008**, *130*, 3619.

23 V. D. Mihailetchi, J. Wildeman, P. W. M. Blom, *Phys. Rev. Lett.* **2005**, *94*, 126602.

24 V. Shrotriya, Y. Yao, G. Li, Y. Yang, *Appl. Phys. Lett.* **2006**, *89*, 063505.

25 H.-Y. Chen, H. Yang, G. Yang, S. Sista, R. Zadoyan, G. Li, Y. Yang, *J. Phys. Chem. C* **2009**, *113*, 7946.